



CERN-EP-2017-190
 LHCb-PAPER-2017-022
 4 December 2017

First observation of the rare purely baryonic decay $B^0 \rightarrow p\bar{p}$

The LHCb collaboration[†]

Abstract

The first observation of the decay of a B^0 meson to a purely baryonic final state, $B^0 \rightarrow p\bar{p}$, is reported. The proton-proton collision data sample used was collected with the LHCb experiment at center-of-mass energies of 7 and 8 TeV and corresponds to an integrated luminosity of 3.0 fb^{-1} . The branching fraction is determined to be

$$\mathcal{B}(B^0 \rightarrow p\bar{p}) = (1.25 \pm 0.27 \pm 0.18) \times 10^{-8},$$

where the first uncertainty is statistical and the second systematic. The decay mode $B^0 \rightarrow p\bar{p}$ is the rarest decay of the B^0 meson observed to date. The decay $B_s^0 \rightarrow p\bar{p}$ is also investigated. No signal is seen and the upper limit $\mathcal{B}(B_s^0 \rightarrow p\bar{p}) < 1.5 \times 10^{-8}$ at 90% confidence level is set on the branching fraction.

Published in Phys. Rev. Lett. 119 (2017) 232001

© CERN on behalf of the LHCb collaboration, licence CC-BY-4.0.

[†]Authors are listed at the end of this Letter.

Studies of B mesons decaying to baryonic final states have been carried out since the late 1990s [1]. It was quickly realized that baryonic and mesonic B -meson decays differ in a number of ways. Two-body baryonic decays are suppressed with respect to decays to multibody final states [2, 3] and the characteristic threshold enhancement in the baryon-antibaryon mass spectrum [4, 5] is still not fully understood. The study of such decays provides information on the dynamics of B decays and tests QCD-based models of the hadronization process [5]. It helps to discriminate the available models and makes it possible to extract both tree and penguin amplitudes of charmless two-body baryonic decays when combining the information on the $B^0 \rightarrow p\bar{p}$ and $B^+ \rightarrow p\bar{\Lambda}$ branching fractions [6].

Baryonic B decays are also interesting in the study of CP violation. First evidence of CP violation in baryonic B decays has been reported from the analysis of $B^+ \rightarrow p\bar{p}K^+$ decays [7] and awaits confirmation in other decay modes [8].

This Letter presents a search for the suppressed decays of B^0 and B_s^0 mesons to the two-body charmless baryonic final state $p\bar{p}$. Prior to searches at the LHC, the ALEPH, CLEO, BaBar and Belle collaborations searched for the $B^0 \rightarrow p\bar{p}$ decay [9–12]. The most stringent upper limit on its branching fraction was obtained by the Belle experiment and is $\mathcal{B}(B^0 \rightarrow p\bar{p}) < 1.1 \times 10^{-7}$ at 90% confidence level (CL) [12]. The only search for the $B_s^0 \rightarrow p\bar{p}$ decay, performed by the ALEPH collaboration, yielded the upper limit $\mathcal{B}(B_s^0 \rightarrow p\bar{p}) < 5.9 \times 10^{-5}$ at 90% CL [9].

The LHCb collaboration has greatly increased the knowledge of baryonic B decays in recent years [7, 13–17]. The collaboration has reported the first observation of a two-body charmless baryonic B^+ decay, $B^+ \rightarrow p\bar{\Lambda}(1520)$ [7], and the first evidence for $B^0 \rightarrow p\bar{p}$, a two-body charmless baryonic decay of the B^0 meson [13]. The experimental data on two-body final states is nevertheless scarce. The study of these suppressed modes requires large data samples that are presently only available at the LHC.

In this analysis, in order to suppress common systematic uncertainties, the branching fractions of the $B^0 \rightarrow p\bar{p}$ and $B_s^0 \rightarrow p\bar{p}$ decays are measured using the topologically identical decay $B^0 \rightarrow K^+\pi^-$. The branching fractions are determined from

$$\mathcal{B}(B_{(s)}^0 \rightarrow p\bar{p}) = \frac{N(B_{(s)}^0 \rightarrow p\bar{p})}{N(B^0 \rightarrow K^+\pi^-)} \frac{\varepsilon_{B^0 \rightarrow K^+\pi^-}}{\varepsilon_{B_{(s)}^0 \rightarrow p\bar{p}}} \mathcal{B}(B^0 \rightarrow K^+\pi^-) \left(\times \frac{f_d}{f_s} \right), \quad (1)$$

where N represents yields determined from fits to the $p\bar{p}$ or $K^+\pi^-$ invariant mass distributions, f_d/f_s (included only for the B_s^0 mode) is the ratio of b -quark hadronization probabilities into the B^0 and B_s^0 mesons [18] and ε represents the geometrical acceptance, reconstruction and selection efficiencies. The notation $B_{(s)}^0 \rightarrow p\bar{p}$ stands for either $B^0 \rightarrow p\bar{p}$ or $B_s^0 \rightarrow p\bar{p}$. The inclusion of charge-conjugate processes is implied, unless otherwise indicated.

The data sample analyzed corresponds to an integrated luminosity of 1.0 fb^{-1} of proton-proton collision data collected by the LHCb experiment at center-of-mass energies of 7 TeV in 2011 and 2.0 fb^{-1} at 8 TeV in 2012. The LHCb detector [19, 20] is a single-arm forward spectrometer covering the pseudorapidity range $2 < \eta < 5$, designed for the study of particles containing b or c quarks. The detector includes a high-precision tracking system consisting of a silicon-strip vertex detector surrounding the pp interaction region [21], a large-area silicon-strip detector located upstream of a dipole magnet with a bending power of about 4 Tm , and three stations of silicon-strip detectors and straw drift tubes [22] placed

downstream of the magnet. The tracking system provides a measurement of momentum, p , of charged particles with a relative uncertainty that varies from 0.5% at low momentum to 1.0% at 200 GeV/ c . The minimum distance of a track to a primary vertex (PV), the impact parameter (IP), is measured with a resolution of $(15 + 29/p_T) \mu\text{m}$, where p_T is the component of the momentum transverse to the beam, in GeV/ c . Different types of charged hadrons are distinguished using information from two ring-imaging Cherenkov detectors [23]. Photons, electrons and hadrons are identified by a calorimeter system consisting of scintillating-pad and preshower detectors, an electromagnetic calorimeter and a hadronic calorimeter. Muons are identified by a system composed of alternating layers of iron and detector planes consisting of multiwire proportional chambers and gas electron multipliers. Simulated data samples, produced as described in Refs. [24–29], are used to evaluate the response of the detector and to investigate and characterize possible sources of background.

Candidates are selected in a similar way for both signal $B_{(s)}^0 \rightarrow p\bar{p}$ decays and the normalization channel $B^0 \rightarrow K^+\pi^-$. Real-time event selection is performed by a trigger [30] consisting of a hardware stage, based on information from the calorimeter and muon systems, followed by a software stage, which performs a full event reconstruction. The hardware trigger stage requires events to have a hadron, photon or electron with high transverse energy (above a few GeV) deposited in the calorimeters, or a muon with high transverse momentum. For this analysis, the hardware trigger decision can be made either on the signal candidates or on other particles in the event. The software trigger requires a two-track secondary vertex with a significant displacement from the PVs. At least one charged particle must have high p_T and be inconsistent with originating from a PV. A multivariate algorithm [31] is used for the identification of secondary vertices consistent with the decay of a b or c hadron.

The final selection of candidates in the signal and normalization modes is carried out with a preselection stage, particle identification (PID) criteria, and a requirement on the response of a multilayer perceptron (MLP) classifier [32]. To avoid potential biases, $p\bar{p}$ candidates with invariant mass in the range [5230, 5417] MeV/ c^2 (a ± 50 MeV/ c^2 window approximately three times the invariant mass resolution around the known B^0 and B_s^0 masses [33]) were not examined until the analysis procedure was finalized.

At the preselection stage, the $B_{(s)}^0$ decay products are associated with tracks with good reconstruction quality that have $\chi_{\text{IP}}^2 > 9$ with respect to any PV, where the χ_{IP}^2 is defined as the difference between the vertex-fit χ^2 of a PV reconstructed with and without the track in question. The minimum p_T of the decay products is required to be above 900 MeV/ c and at least one of the decay products is required to have $p_T > 2100$ MeV/ c . A loose PID requirement, based primarily on information from the Cherenkov detectors, is also imposed on both particles. The $B_{(s)}^0$ candidate must have a vertex with good reconstruction quality, $p_T > 1000$ MeV/ c and a $\chi_{\text{IP}}^2 < 36$ with respect to the associated PV. The associated PV is that with which it forms the smallest χ_{IP}^2 . The angle θ_B between the momentum vector of the $B_{(s)}^0$ candidate and the line connecting the associated PV and the candidate's decay vertex is required to be close to zero ($\cos(\theta_B) > 0.9995$).

After preselection, tight PID requirements are applied to the two final-state particles to suppress so-called combinatorial background formed from the accidental associations of tracks unrelated to the signal decays, and to reduce contamination from b -hadron decays where one or more decay products are misidentified. The PID requirements are determined by optimizing the figure of merit $\varepsilon^{\text{sig}} / (\frac{a}{2} + \sqrt{N_{\text{bkg}}})$ [34], where $a = 5$ quantifies

the target level of significance in standard deviations and ε^{sig} is the PID efficiency of the signal selection. The quantity N_{bkg} denotes the expected number of background events in the signal region. This is estimated by extrapolating the result of a fit to the invariant mass distribution of the data in the sideband regions above and below the signal region. The PID criteria are allowed to be different for protons and antiprotons. The optimization of the PID criteria applied to the normalization decay candidates relies on maximizing the signal significance, while minimizing the contamination from misidentified backgrounds.

Further separation between signal and combinatorial background candidates relies on an MLP implemented with the TMVA toolkit [35]. There are ten input quantities to the MLP classifier: the minimum values of the p_{T} and η of the decay products, the scalar sum of their p_{T} values, the χ^2_{IP} of the decay products; the distance of closest approach between the two decay products; a parameter expressing the quality of the $B_{(s)}^0$ vertex fit; the χ^2_{IP} and θ_B angle of the $B_{(s)}^0$ candidate; and the p_{T} asymmetry within a cone around the $B_{(s)}^0$ direction defined by $A_{p_{\text{T}}} = (p_{\text{T}}^B - p_{\text{T}}^{\text{cone}})/(p_{\text{T}}^B + p_{\text{T}}^{\text{cone}})$, where $p_{\text{T}}^{\text{cone}}$ is the transverse component of the vector sum of the momenta of all tracks measured within the cone radius $R = 1.0$ around the $B_{(s)}^0$ direction, except for the $B_{(s)}^0$ decay products. The cone radius is defined in pseudorapidity and azimuthal angle (η, ϕ) as $R = \sqrt{(\Delta\eta)^2 + (\Delta\phi)^2}$. The $A_{p_{\text{T}}}$ requirement exploits the relative isolation of signal decay products as compared with background. The MLP is trained using simulated $B^0 \rightarrow p\bar{p}$ decays and data candidates in the $p\bar{p}$ invariant mass sideband above $5417 \text{ MeV}/c^2$ to represent the background. The requirement on the MLP response is optimized using the same figure of merit as that used for the optimization of the PID selection. The MLP selection keeps approximately 60% of the signal candidates, while suppressing combinatorial background by two orders of magnitude. The MLP applied to the normalization decay candidates is the same as that trained to select the $B_{(s)}^0 \rightarrow p\bar{p}$ signal candidates, with the requirement on the response chosen to maximize the $B^0 \rightarrow K^+\pi^-$ significance. A vanishingly small fraction of events contains a second candidate after all selection requirements are applied and all candidates are kept.

Large control data samples of kinematically identified pions, kaons and protons originating from the decays $D^0 \rightarrow K^-\pi^+$, $\Lambda \rightarrow p\pi^-$ and $\Lambda_c^+ \rightarrow pK^-\pi^+$ are employed to determine the efficiency of the PID requirements [23]. All the other components of the selection efficiencies are determined from simulation. The agreement between data and simulation is verified comparing kinematic distributions from selected $B^0 \rightarrow K^+\pi^-$ decays. The distributions in data are obtained with the *sPlot* technique [36] with the B^0 candidate invariant mass used as the discriminating variable. The overall efficiencies of this analysis, including the trigger selection and the reconstruction, are of the order 10^{-3} .

Sources of noncombinatorial background to the $p\bar{p}$ spectrum are investigated using simulation samples. These sources include partially reconstructed backgrounds in which one or more particles from the decay of a b hadron are not associated with the signal candidate, or b -hadron decays where one or more decay products are misidentified. The sum of such backgrounds does not peak in the B^0 and B_s^0 signal regions but rather contributes a smooth $p\bar{p}$ mass spectrum, which is indistinguishable from the dominant combinatorial background.

The yields of the signal and normalization candidates are determined using unbinned maximum likelihood fits to the invariant mass distributions. The $p\bar{p}$ invariant mass distribution is described with three components, namely the $B^0 \rightarrow p\bar{p}$ and $B_s^0 \rightarrow p\bar{p}$ signals and combinatorial background. The $B_{(s)}^0 \rightarrow p\bar{p}$ signals are modeled with the sum of two

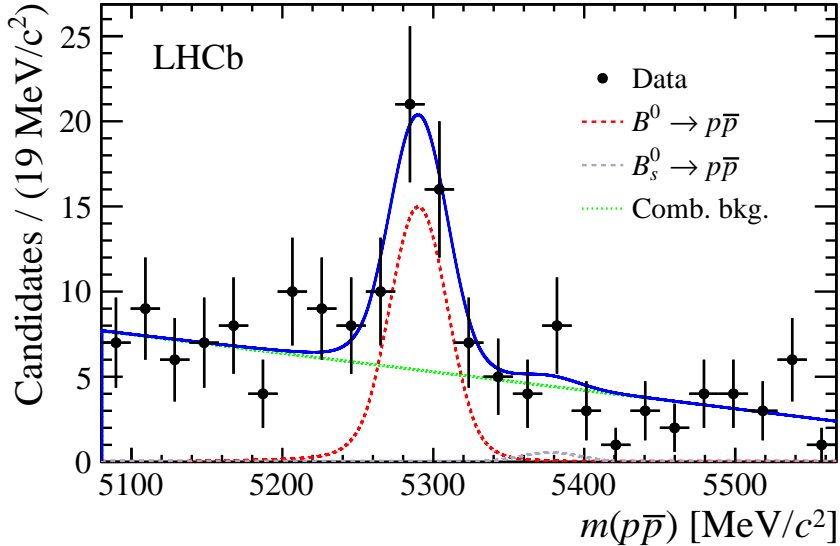


Figure 1: Invariant mass distribution of $p\bar{p}$ candidates. The fit result (blue, solid line) is shown together with each fit model component: the $B^0 \rightarrow p\bar{p}$ signal (red, dashed line), the $B_s^0 \rightarrow p\bar{p}$ signal (grey, dashed line) and the combinatorial background (green, dotted line).

Crystal Ball (CB) functions [37] describing the high- and low-mass asymmetric tails. The two components of each signal share the same peak and core width parameters. The core widths are fixed using $B_{(s)}^0 \rightarrow p\bar{p}$ simulated samples. A scaling factor is applied to account for differences in the resolution between data and simulation as determined from $B^0 \rightarrow K^+\pi^-$ candidates. The $B_s^0 \rightarrow p\bar{p}$ signal peak value is set relative to the $B^0 \rightarrow p\bar{p}$ signal peak value determined from the fit according to the B_s^0 - B^0 mass difference [33]. The tail parameters and the relative normalization of the CB functions are determined from simulation. The combinatorial background is described with a linear function, with the slope parameter allowed to vary in the fit.

The $p\bar{p}$ invariant mass distribution is presented in Fig. 1 together with the result of the fit. The yields of the $B_{(s)}^0 \rightarrow p\bar{p}$ signals are $N(B^0 \rightarrow p\bar{p}) = 39 \pm 8$ and $N(B_s^0 \rightarrow p\bar{p}) = 2 \pm 4$, where the uncertainties are statistical only. The significance of each of the signals is determined from the change in the logarithm of the likelihood between fits with and without the signal component [38]. The $B^0 \rightarrow p\bar{p}$ decay mode is found to have a significance of 5.3 standard deviations, including systematic uncertainties, and the $B_s^0 \rightarrow p\bar{p}$ mode is found to have a significance of 0.4 standard deviations, where, given its size, the significance has been evaluated ignoring systematic effects. The high significance of the $B^0 \rightarrow p\bar{p}$ signal implies the first observation of a two-body charmless baryonic B^0 decay.

The $K^+\pi^-$ invariant mass distribution of the normalization decay candidates is described with components accounting for the $B^0 \rightarrow K^+\pi^-$ and $B_s^0 \rightarrow \pi^+K^-$ signals; the background due to the decays $B^0 \rightarrow \pi^+\pi^-$, $B_s^0 \rightarrow K^+K^-$, $\Lambda_b^0 \rightarrow p\pi^-$ and $\Lambda_b^0 \rightarrow pK^-$ when at least one of the final-state particles is misidentified; background from partially reconstructed b -hadron decays; and combinatorial background. The $B^0 \rightarrow K^+\pi^-$ and $B_s^0 \rightarrow \pi^+K^-$ decays are modeled with the sum of two CB functions sharing the same peak and core width parameters. The peak value and core width of the $B^0 \rightarrow K^+\pi^-$ signal model are free parameters in the fit. The difference between the peak positions of

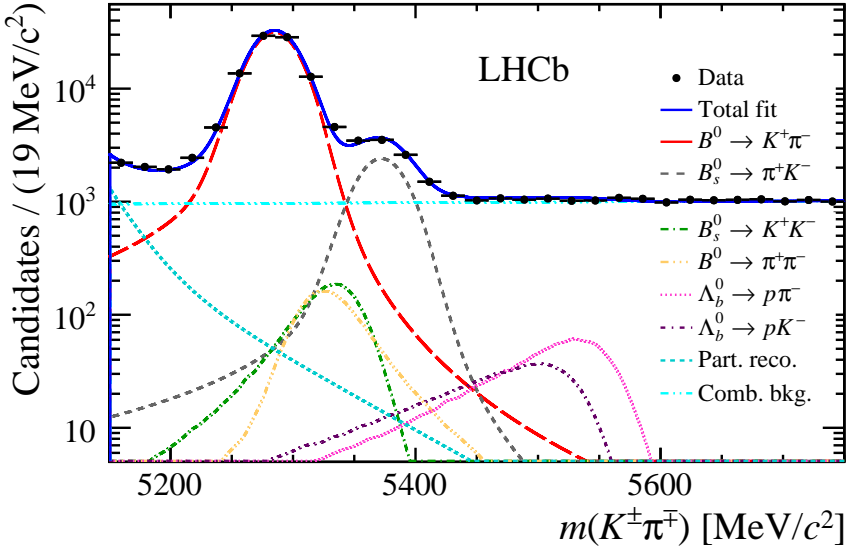


Figure 2: Invariant mass distribution of $K^\pm\pi^\mp$ candidates. The fit result (blue, solid line) is shown together with each fit model component.

the $B^0 \rightarrow K^+\pi^-$ and $B_s^0 \rightarrow \pi^+K^-$ signals is constrained to its known value [33] and the core width of the $B_s^0 \rightarrow \pi^+K^-$ signal is related to the $B^0 \rightarrow K^+\pi^-$ signal core width by a scaling factor of 1.02 as determined from simulation. The tail parameters and the relative normalization of both double CB functions are determined from simulation. The invariant mass distributions of the four misidentified decays are determined from simulation and are modeled with nonparametric functions [39]. The relative fractions of these background components depend upon the branching fractions, b -hadron hadronization probabilities and misidentification rates of the backgrounds. The fractions are Gaussian-constrained to the product of these three factors, with the widths of the Gaussian functions equal to their combined uncertainties. The misidentification rates are determined from calibration data samples, whereas all other selection efficiencies are obtained from simulation. Partially reconstructed backgrounds represent decay modes misreconstructed as signal with one or more undetected final-state particles, possibly in conjunction with misidentifications. The shapes of these backgrounds in $K^+\pi^-$ invariant mass are determined from simulation, where each contributing decay is assigned a weight dependent on its relative branching fraction, hadronization probability and selection efficiency. The weighted sum of the partially reconstructed backgrounds is well modeled with the sum of two exponential functions, the slope parameters of which are fixed from simulation, while the yield is determined in the fit to the data. As for the signal fit, the combinatorial background is described with a linear function, with the slope parameter allowed to vary in the fit.

The fit to the $K^+\pi^-$ invariant mass, shown in Fig. 2, involves seven fitted parameters and yields $N(B^0 \rightarrow K^+\pi^-) = 88\,961 \pm 341$ signal decays, where the uncertainty is statistical only.

The sources of systematic uncertainty on the $B_{(s)}^0 \rightarrow p\bar{p}$ branching fractions arise from the fit model, the limited knowledge of the selection efficiencies, and the uncertainties on the $B^0 \rightarrow K^+\pi^-$ branching fraction and on the ratio of b -quark hadronization probabilities f_s/f_d . Pseudoexperiments are used to estimate the effects of using alternative shapes

for the fit components and of including additional backgrounds in the fit. Systematic uncertainties on the fit models are also assessed by varying the fixed parameters of the models within their uncertainties. The description of the combinatorial background is replaced by an exponential function. In the fit to the signal modes, the partially reconstructed decays $B^+ \rightarrow p\bar{p}\ell^+\bar{\nu}_\ell$, where ℓ stands for an electron or a muon and ν_ℓ for the corresponding neutrino, are added to the fit model. Intrinsic biases in the fitted yields are also investigated with pseudoexperiments and are found to be negligible.

Uncertainties on the efficiencies arise from residual differences between data and simulation in the trigger, reconstruction, selection and uncertainties on the data-driven particle identification efficiencies. These differences are assessed using the $B^0 \rightarrow K^+\pi^-$ normalization decay, comparing the level of agreement between simulation and data. The distributions of selection variables for $B^0 \rightarrow K^+\pi^-$ signal candidates in data are obtained by subtracting the background using the *sPlot* technique [36], with the $K^+\pi^-$ candidate invariant mass as the discriminating variable. The effect of binning the PID calibration samples used to obtain the PID efficiencies is evaluated by varying the binning scheme and by adding an extra dimension accounting for event multiplicity to the binning of the samples.

The uncertainty on the branching fraction of the normalization decay, $\mathcal{B}(B^0 \rightarrow K^+\pi^-) = (1.96 \pm 0.05) \times 10^{-5}$ [33], is taken as a systematic uncertainty from external inputs. The uncertainty on the measurement $f_s/f_d = 0.259 \pm 0.015$ [18] is quoted as a separate source of systematic uncertainty from external inputs in the determination of the upper limit on $\mathcal{B}(B_s^0 \rightarrow p\bar{p})$. The total systematic uncertainty on the $B^0 \rightarrow p\bar{p}$ ($B_s^0 \rightarrow p\bar{p}$) branching fraction is given by the sum of all uncertainties added in quadrature and amounts to 14.2% (209%). The systematic uncertainties on the $B^0 \rightarrow p\bar{p}$ ($B_s^0 \rightarrow p\bar{p}$) branching fraction are dominated by the uncertainties on the fit model, which are 7.3% (208%), and on the reconstruction and selection efficiencies, which amount to 6.1% (6.1%) and 8.6% (8.3%), respectively. Specifically, the systematic uncertainty arising from the description of the fit model backgrounds dominates the uncertainty on the $B_s^0 \rightarrow p\bar{p}$ branching fraction.

In summary, the first observation of the simplest decay of a B^0 meson to a purely baryonic final state, $B^0 \rightarrow p\bar{p}$, is reported using a data sample of proton-proton collisions collected with the LHCb experiment, corresponding to a total integrated luminosity of 3.0 fb^{-1} . This rare two-body charmless baryonic decay is observed with a significance of 5.3 standard deviations, including systematic uncertainties. The $B^0 \rightarrow p\bar{p}$ branching fraction is determined to be

$$\mathcal{B}(B^0 \rightarrow p\bar{p}) = (1.25 \pm 0.27 \pm 0.18) \times 10^{-8},$$

where the first uncertainty is statistical and the second systematic. Since no $B_s^0 \rightarrow p\bar{p}$ signal is seen, the world's best upper limit $\mathcal{B}(B_s^0 \rightarrow p\bar{p}) < 1.5 \times 10^{-8}$ at 90% confidence level is set on the decay branching fraction using the Feldman-Cousins frequentist method [40].

The first observation of the decay $B^0 \rightarrow p\bar{p}$, the rarest B^0 decay ever observed, provides valuable input towards the understanding of the dynamics of hadronic B decays. This measurement helps to discriminate among several QCD-based models and makes it possible to extract both tree and penguin amplitudes of charmless two-body baryonic decays when combining the information on the $B^0 \rightarrow p\bar{p}$ and $B^+ \rightarrow p\bar{\Lambda}$ branching fractions [6]. The measured $B^0 \rightarrow p\bar{p}$ branching fraction is compatible with recent theoretical calculations, as is the upper limit on the $B_s^0 \rightarrow p\bar{p}$ branching fraction [2, 3, 6]. An improved measurement

of the $B_s^0 \rightarrow p\bar{p}$ branching fraction will make it possible to quantitatively compare the models proposed in Refs. [2] and [6].

Acknowledgements

We express our gratitude to our colleagues in the CERN accelerator departments for the excellent performance of the LHC. We thank the technical and administrative staff at the LHCb institutes. We acknowledge support from CERN and from the national agencies: CAPES, CNPq, FAPERJ and FINEP (Brazil); MOST and NSFC (China); CNRS/IN2P3 (France); BMBF, DFG and MPG (Germany); INFN (Italy); NWO (The Netherlands); MNiSW and NCN (Poland); MEN/IFA (Romania); MinES and FASO (Russia); MinECo (Spain); SNSF and SER (Switzerland); NASU (Ukraine); STFC (United Kingdom); NSF (USA). We acknowledge the computing resources that are provided by CERN, IN2P3 (France), KIT and DESY (Germany), INFN (Italy), SURF (The Netherlands), PIC (Spain), GridPP (United Kingdom), RRCKI and Yandex LLC (Russia), CSCS (Switzerland), IFIN-HH (Romania), CBPF (Brazil), PL-GRID (Poland) and OSC (USA). We are indebted to the communities behind the multiple open-source software packages on which we depend. Individual groups or members have received support from AvH Foundation (Germany), EPLANET, Marie Skłodowska-Curie Actions and ERC (European Union), ANR, Labex P2IO, ENIGMASS and OCEVU, and Région Auvergne-Rhône-Alpes (France), RFBR and Yandex LLC (Russia), GVA, XuntaGal and GENCAT (Spain), Herchel Smith Fund, the Royal Society, the English-Speaking Union and the Leverhulme Trust (United Kingdom).

References

- [1] CLEO collaboration, X. Fu *et al.*, *Observation of exclusive B decays to final states containing a charmed baryon*, Phys. Rev. Lett. **79** (1997) 3125.
- [2] Y. K. Hsiao and C. Q. Geng, *Violation of partial conservation of the axial-vector current and two-body baryonic B and D_s decays*, Phys. Rev. **D91** (2015) 077501, [arXiv:1407.7639](https://arxiv.org/abs/1407.7639).
- [3] H.-Y. Cheng and C.-K. Chua, *On the smallness of tree-dominated charmless two-body baryonic B decay rates*, Phys. Rev. **D91** (2015) 036003, [arXiv:1412.8272](https://arxiv.org/abs/1412.8272).
- [4] W.-S. Hou and A. Soni, *Pathways to rare baryonic B decays*, Phys. Rev. Lett. **86** (2001) 4247, [arXiv:hep-ph/0008079](https://arxiv.org/abs/hep-ph/0008079).
- [5] BaBar and Belle collaborations, A. J. Bevan *et al.*, *The physics of the B factories*, Eur. Phys. J. **C74** (2014) 3026, [arXiv:1406.6311](https://arxiv.org/abs/1406.6311).
- [6] C.-K. Chua, *Rates and CP asymmetries of charmless two-body baryonic $B_{u,d,s}$ decays*, Phys. Rev. **D95** (2017) 096004, [arXiv:1612.04249](https://arxiv.org/abs/1612.04249).
- [7] LHCb collaboration, R. Aaij *et al.*, *Evidence for CP violation in $B^+ \rightarrow p\bar{p}K^+$ decays*, Phys. Rev. Lett. **113** (2014) 141801, [arXiv:1407.5907](https://arxiv.org/abs/1407.5907).

- [8] C. Q. Geng, Y. K. Hsiao, and J. N. Ng, *Direct CP violation in $B^\pm \rightarrow p\bar{p}K^{(*)\pm}$* , Phys. Rev. Lett. **98** (2007) 011801, [arXiv:hep-ph/0608328](#).
- [9] ALEPH collaboration, D. Buskulic *et al.*, *Observation of charmless hadronic B decays*, Phys. Lett. **B384** (1996) 471.
- [10] CLEO collaboration, T. E. Coan *et al.*, *Search for exclusive rare baryonic decays of B mesons*, Phys. Rev. **D59** (1999) 111101, [arXiv:hep-ex/9810043](#).
- [11] BaBar collaboration, B. Aubert *et al.*, *Search for the decay $B^0 \rightarrow p\bar{p}$* , Phys. Rev. **D69** (2004) 091503, [arXiv:hep-ex/0403003](#).
- [12] Belle collaboration, Y.-T. Tsai *et al.*, *Search for $B^0 \rightarrow p\bar{p}, \Lambda\bar{\Lambda}$ and $B^+ \rightarrow p\bar{\Lambda}$ at Belle*, Phys. Rev. **D75** (2007) 111101, [arXiv:hep-ex/0703048](#).
- [13] LHCb collaboration, R. Aaij *et al.*, *First evidence for the two-body charmless baryonic decay $B^0 \rightarrow p\bar{p}$* , JHEP **10** (2013) 005, [arXiv:1308.0961](#).
- [14] LHCb collaboration, R. Aaij *et al.*, *First observation of a baryonic B_c^+ decay*, Phys. Rev. Lett. **113** (2014) 152003, [arXiv:1408.0971](#).
- [15] LHCb collaboration, R. Aaij *et al.*, *Evidence for the two-body charmless baryonic decay $B^+ \rightarrow p\bar{\Lambda}$* , JHEP **04** (2017) 162, [arXiv:1611.07805](#).
- [16] LHCb collaboration, R. Aaij *et al.*, *First observation of a baryonic B_s^0 decay*, Phys. Rev. Lett. **119** (2017) 041802, [arXiv:1704.07908](#).
- [17] LHCb collaboration, R. Aaij *et al.*, *Observation of charmless baryonic decays $B_{(s)}^0 \rightarrow p\bar{p}h^+h^-$* , [arXiv:1704.08497](#), submitted to Phys. Rev. D.
- [18] LHCb collaboration, R. Aaij *et al.*, *Measurement of the fragmentation fraction ratio f_s/f_d and its dependence on B meson kinematics*, JHEP **04** (2013) 001, [arXiv:1301.5286](#), f_s/f_d value updated in LHCb-CONF-2013-011.
- [19] LHCb collaboration, A. A. Alves Jr. *et al.*, *The LHCb detector at the LHC*, JINST **3** (2008) S08005.
- [20] LHCb collaboration, R. Aaij *et al.*, *LHCb detector performance*, Int. J. Mod. Phys. **A30** (2015) 1530022, [arXiv:1412.6352](#).
- [21] R. Aaij *et al.*, *Performance of the LHCb Vertex Locator*, JINST **9** (2014) P09007, [arXiv:1405.7808](#).
- [22] R. Arink *et al.*, *Performance of the LHCb Outer Tracker*, JINST **9** (2014) P01002, [arXiv:1311.3893](#).
- [23] M. Adinolfi *et al.*, *Performance of the LHCb RICH detector at the LHC*, Eur. Phys. J. **C73** (2013) 2431, [arXiv:1211.6759](#).
- [24] T. Sjöstrand, S. Mrenna, and P. Skands, *A brief introduction to PYTHIA 8.1*, Comput. Phys. Commun. **178** (2008) 852, [arXiv:0710.3820](#); T. Sjöstrand, S. Mrenna, and P. Skands, *PYTHIA 6.4 physics and manual*, JHEP **05** (2006) 026, [arXiv:hep-ph/0603175](#).

- [25] I. Belyaev *et al.*, *Handling of the generation of primary events in Gauss, the LHCb simulation framework*, J. Phys. Conf. Ser. **331** (2011) 032047.
- [26] D. J. Lange, *The EvtGen particle decay simulation package*, Nucl. Instrum. Meth. **A462** (2001) 152.
- [27] P. Golonka and Z. Was, *PHOTOS Monte Carlo: A precision tool for QED corrections in Z and W decays*, Eur. Phys. J. **C45** (2006) 97, [arXiv:hep-ph/0506026](https://arxiv.org/abs/hep-ph/0506026).
- [28] Geant4 collaboration, J. Allison *et al.*, *Geant4 developments and applications*, IEEE Trans. Nucl. Sci. **53** (2006) 270; Geant4 collaboration, S. Agostinelli *et al.*, *Geant4: A simulation toolkit*, Nucl. Instrum. Meth. **A506** (2003) 250.
- [29] M. Clemencic *et al.*, *The LHCb simulation application, Gauss: Design, evolution and experience*, J. Phys. Conf. Ser. **331** (2011) 032023.
- [30] R. Aaij *et al.*, *The LHCb trigger and its performance in 2011*, JINST **8** (2013) P04022, [arXiv:1211.3055](https://arxiv.org/abs/1211.3055).
- [31] V. V. Gligorov and M. Williams, *Efficient, reliable and fast high-level triggering using a bonsai boosted decision tree*, JINST **8** (2013) P02013, [arXiv:1210.6861](https://arxiv.org/abs/1210.6861).
- [32] D. E. Rumelhart, G. E. Hinton, and R. J. Williams, *Parallel distributed processing: explorations in the microstructure of cognition*, vol. 1, MIT, Cambridge, USA, 1986.
- [33] Particle Data Group, C. Patrignani *et al.*, *Review of particle physics*, Chin. Phys. **C40** (2016) 100001.
- [34] G. Punzi, *Sensitivity of searches for new signals and its optimization*, in *Statistical Problems in Particle Physics, Astrophysics, and Cosmology* (L. Lyons, R. Mount, and R. Reitmeyer, eds.), p. 79, 2003. [arXiv:physics/0308063](https://arxiv.org/abs/physics/0308063).
- [35] P. Speckmayer, A. Hoecker, J. Stelzer, and H. Voss, *The toolkit for multivariate data analysis: TMVA 4*, J. Phys. Conf. Ser. **219** (2010) 032057.
- [36] M. Pivk and F. R. Le Diberder, *sPlot: A statistical tool to unfold data distributions*, Nucl. Instrum. Meth. **A555** (2005) 356, [arXiv:physics/0402083](https://arxiv.org/abs/physics/0402083).
- [37] T. Skwarnicki, *A study of the radiative cascade transitions between the Upsilon-prime and Upsilon resonances*, PhD thesis, Institute of Nuclear Physics, Krakow, 1986, DESY-F31-86-02.
- [38] S. S. Wilks, *The large-sample distribution of the likelihood ratio for testing composite hypotheses*, Ann. Math. Stat. **9** (1938) 60.
- [39] K. S. Cranmer, *Kernel estimation in high-energy physics*, Comput. Phys. Commun. **136** (2001) 198, [arXiv:hep-ex/0011057](https://arxiv.org/abs/hep-ex/0011057).
- [40] G. J. Feldman and R. D. Cousins, *Unified approach to the classical statistical analysis of small signals*, Phys. Rev. **D57** (1998) 3873.

LHCb collaboration

R. Aaij⁴⁰, B. Adeva³⁹, M. Adinolfi⁴⁸, Z. Ajaltouni⁵, S. Akar⁵⁹, J. Albrecht¹⁰, F. Alessio⁴⁰, M. Alexander⁵³, A. Alfonso Albero³⁸, S. Ali⁴³, G. Alkhazov³¹, P. Alvarez Cartelle⁵⁵, A.A. Alves Jr⁵⁹, S. Amato², S. Amerio²³, Y. Amhis⁷, L. An³, L. Anderlini¹⁸, G. Andreassi⁴¹, M. Andreotti^{17,g}, J.E. Andrews⁶⁰, R.B. Appleby⁵⁶, F. Archilli⁴³, P. d'Argent¹², J. Arnau Romeu⁶, A. Artamonov³⁷, M. Artuso⁶¹, E. Aslanides⁶, G. Auriemma²⁶, M. Baalouch⁵, I. Babuschkin⁵⁶, S. Bachmann¹², J.J. Back⁵⁰, A. Badalov^{38,m}, C. Baesso⁶², S. Baker⁵⁵, V. Balagura^{7,b}, W. Baldini¹⁷, A. Baranov³⁵, R.J. Barlow⁵⁶, C. Barschel⁴⁰, S. Barsuk⁷, W. Barter⁵⁶, F. Baryshnikov³², V. Batozskaya²⁹, V. Battista⁴¹, A. Bay⁴¹, L. Beaucourt⁴, J. Beddow⁵³, F. Bedeschi²⁴, I. Bediaga¹, A. Beiter⁶¹, L.J. Bel⁴³, N. Beliy⁶³, V. Bellee⁴¹, N. Belloli^{21,i}, K. Belous³⁷, I. Belyaev³², E. Ben-Haim⁸, G. Bencivenni¹⁹, S. Benson⁴³, S. Beranek⁹, A. Berezhnoy³³, R. Bernet⁴², D. Berninghoff¹², E. Bertholet⁸, A. Bertolin²³, C. Betancourt⁴², F. Betti¹⁵, M.-O. Bettler⁴⁰, M. van Beuzekom⁴³, Ia. Bezshyiko⁴², S. Bifani⁴⁷, P. Billoir⁸, A. Birnkraut¹⁰, A. Bitadze⁵⁶, A. Bizzeti^{18,u}, M. Bjørn⁵⁷, T. Blake⁵⁰, F. Blanc⁴¹, J. Blouw^{11,†}, S. Blusk⁶¹, V. Bocci²⁶, T. Boettcher⁵⁸, A. Bondar^{36,w}, N. Bondar³¹, W. Bonivento¹⁶, I. Bordyuzhin³², A. Borgheresi^{21,i}, S. Borghi⁵⁶, M. Boris'yak³⁵, M. Borsato³⁹, F. Bossu⁷, M. Boubdir⁹, T.J.V. Bowcock⁵⁴, E. Bowen⁴², C. Bozzi^{17,40}, S. Braun¹², T. Britton⁶¹, J. Brodzicka²⁷, D. Brundu¹⁶, E. Buchanan⁴⁸, C. Burr⁵⁶, A. Bursche^{16,f}, J. Buytaert⁴⁰, W. Byczynski⁴⁰, S. Cadeddu¹⁶, H. Cai⁶⁴, R. Calabrese^{17,g}, R. Calladine⁴⁷, M. Calvi^{21,i}, M. Calvo Gomez^{38,m}, A. Camboni^{38,m}, P. Campana¹⁹, D.H. Campora Perez⁴⁰, L. Capriotti⁵⁶, A. Carbone^{15,e}, G. Carboni^{25,j}, R. Cardinale^{20,h}, A. Cardini¹⁶, P. Carniti^{21,i}, L. Carson⁵², K. Carvalho Akiba², G. Casse⁵⁴, L. Cassina²¹, L. Castillo Garcia⁴¹, M. Cattaneo⁴⁰, G. Cavallero^{20,40,h}, R. Cenci^{24,t}, D. Chamont⁷, M. Charles⁸, Ph. Charpentier⁴⁰, G. Chatzikonstantinidis⁴⁷, M. Chefdeville⁴, S. Chen⁵⁶, S.F. Cheung⁵⁷, S.-G. Chitic⁴⁰, V. Chobanova³⁹, M. Chrzaszcz^{42,27}, A. Chubykin³¹, P. Ciambrone¹⁹, X. Cid Vidal³⁹, G. Ciezarek⁴³, P.E.L. Clarke⁵², M. Clemencic⁴⁰, H.V. Cliff⁴⁹, J. Closier⁴⁰, J. Cogan⁶, E. Cogneras⁵, V. Cogoni^{16,f}, L. Cojocariu³⁰, P. Collins⁴⁰, T. Colombo⁴⁰, A. Comerma-Montells¹², A. Contu⁴⁰, A. Cook⁴⁸, G. Coombs⁴⁰, S. Coquereau³⁸, G. Corti⁴⁰, M. Corvo^{17,g}, C.M. Costa Sobral⁵⁰, B. Couturier⁴⁰, G.A. Cowan⁵², D.C. Craik⁵⁸, A. Crocombe⁵⁰, M. Cruz Torres¹, R. Currie⁵², C. D'Ambrosio⁴⁰, F. Da Cunha Marinho², E. Dall'Occo⁴³, J. Dalseno⁴⁸, A. Davis³, O. De Aguiar Francisco⁵⁴, S. De Capua⁵⁶, M. De Cian¹², J.M. De Miranda¹, L. De Paula², M. De Serio^{14,d}, P. De Simone¹⁹, C.T. Dean⁵³, D. Decamp⁴, L. Del Buono⁸, H.-P. Dembinski¹¹, M. Demmer¹⁰, A. Dendek²⁸, D. Derkach³⁵, O. Deschamps⁵, F. Dettori⁵⁴, B. Dey⁶⁵, A. Di Canto⁴⁰, P. Di Nezza¹⁹, H. Dijkstra⁴⁰, F. Dordei⁴⁰, M. Dorigo⁴⁰, A. Dosil Suárez³⁹, L. Douglas⁵³, A. Dovbnya⁴⁵, K. Dreimanis⁵⁴, L. Dufour⁴³, G. Dujany⁸, P. Durante⁴⁰, R. Dzhelyadin³⁷, M. Dziewiecki¹², A. Dziurda⁴⁰, A. Dzyuba³¹, S. Easo⁵¹, M. Ebert⁵², U. Egede⁵⁵, V. Egorychev³², S. Eidelman^{36,w}, S. Eisenhardt⁵², U. Eitschberger¹⁰, R. Ekelhof¹⁰, L. Eklund⁵³, S. Ely⁶¹, S. Esen¹², H.M. Evans⁴⁹, T. Evans⁵⁷, A. Falabella¹⁵, N. Farley⁴⁷, S. Farry⁵⁴, D. Fazzini^{21,i}, L. Federici²⁵, D. Ferguson⁵², G. Fernandez³⁸, P. Fernandez Declara⁴⁰, A. Fernandez Prieto³⁹, F. Ferrari¹⁵, F. Ferreira Rodrigues², M. Ferro-Luzzi⁴⁰, S. Filippov³⁴, R.A. Fini¹⁴, M. Fiore^{17,g}, M. Fiorini^{17,g}, M. Firlej²⁸, C. Fitzpatrick⁴¹, T. Fiutowski²⁸, F. Fleuret^{7,b}, K. Fohl⁴⁰, M. Fontana^{16,40}, F. Fontanelli^{20,h}, D.C. Forshaw⁶¹, R. Forty⁴⁰, V. Franco Lima⁵⁴, M. Frank⁴⁰, C. Frei⁴⁰, J. Fu^{22,q}, W. Funk⁴⁰, E. Furfarò^{25,j}, C. Färber⁴⁰, E. Gabriel⁵², A. Gallas Torreira³⁹, D. Galli^{15,e}, S. Gallorini²³, S. Gambetta⁵², M. Gandelman², P. Gandini⁵⁷, Y. Gao³, L.M. Garcia Martin⁷⁰, J. García Pardiñas³⁹, J. Garra Tico⁴⁹, L. Garrido³⁸, P.J. Garsed⁴⁹, D. Gascon³⁸, C. Gaspar⁴⁰, L. Gavardi¹⁰, G. Gazzoni⁵, D. Gerick¹², E. Gersabeck¹², M. Gersabeck⁵⁶, T. Gershon⁵⁰, Ph. Ghez⁴, S. Gianì⁴¹, V. Gibson⁴⁹, O.G. Girard⁴¹, L. Giubega³⁰, K. Gizzdov⁵², V.V. Gligorov⁸, D. Golubkov³², A. Golutvin^{55,40}, A. Gomes^{1,a}, I.V. Gorelov³³, C. Gotti^{21,i}, E. Govorkova⁴³,

J.P. Grabowski¹², R. Graciani Diaz³⁸, L.A. Granado Cardoso⁴⁰, E. Graugés³⁸, E. Graverini⁴²,
 G. Graziani¹⁸, A. Grecu³⁰, R. Greim⁹, P. Griffith¹⁶, L. Grillo^{21,40,i}, L. Gruber⁴⁰,
 B.R. Gruberg Cazon⁵⁷, O. Grünberg⁶⁷, E. Gushchin³⁴, Yu. Guz³⁷, T. Gys⁴⁰, C. Göbel⁶²,
 T. Hadavizadeh⁵⁷, C. Hadjivasilou⁵, G. Haefeli⁴¹, C. Haen⁴⁰, S.C. Haines⁴⁹, B. Hamilton⁶⁰,
 X. Han¹², T.H. Hancock⁵⁷, S. Hansmann-Menzemer¹², N. Harnew⁵⁷, S.T. Harnew⁴⁸,
 J. Harrison⁵⁶, C. Hasse⁴⁰, M. Hatch⁴⁰, J. He⁶³, M. Hecker⁵⁵, K. Heinicke¹⁰, A. Heister⁹,
 K. Hennessy⁵⁴, P. Henrard⁵, L. Henry⁷⁰, E. van Herwijken⁴⁰, M. Heß⁶⁷, A. Hicheur², D. Hill⁵⁷,
 C. Hombach⁵⁶, P.H. Hopchev⁴¹, Z.C. Huard⁵⁹, W. Hulsbergen⁴³, T. Humair⁵⁵, M. Hushchyn³⁵,
 D. Hutchcroft⁵⁴, P. Ibis¹⁰, M. Idzik²⁸, P. Ilten⁵⁸, R. Jacobsson⁴⁰, J. Jalocha⁵⁷, E. Jans⁴³,
 A. Jawahery⁶⁰, F. Jiang³, M. John⁵⁷, D. Johnson⁴⁰, C.R. Jones⁴⁹, C. Joram⁴⁰, B. Jost⁴⁰,
 N. Jurik⁵⁷, S. Kandybei⁴⁵, M. Karacson⁴⁰, J.M. Kariuki⁴⁸, S. Karodia⁵³, N. Kazeev³⁵,
 M. Kecke¹², M. Kelsey⁶¹, M. Kenzie⁴⁹, T. Ketel⁴⁴, E. Khairullin³⁵, B. Khanji¹²,
 C. Khurewathanakul⁴¹, T. Kirn⁹, S. Klaver⁵⁶, K. Klimaszewski²⁹, T. Klimkovich¹¹, S. Koliiev⁴⁶,
 M. Kolpin¹², I. Komarov⁴¹, R. Kopecna¹², P. Koppenburg⁴³, A. Kosmyntseva³²,
 S. Kotriakhova³¹, M. Kozeiha⁵, L. Kravchuk³⁴, M. Kreps⁵⁰, P. Krokovny^{36,w}, F. Kruse¹⁰,
 W. Krzemien²⁹, W. Kucewicz^{27,l}, M. Kucharczyk²⁷, V. Kudryavtsev^{36,w}, A.K. Kuonen⁴¹,
 K. Kurek²⁹, T. Kvaratskhelia^{32,40}, D. Lacarrere⁴⁰, G. Lafferty⁵⁶, A. Lai¹⁶, G. Lanfranchi¹⁹,
 C. Langenbruch⁹, T. Latham⁵⁰, C. Lazzeroni⁴⁷, R. Le Gac⁶, A. Leflat^{33,40}, J. Lefrançois⁷,
 R. Lefevre⁵, F. Lemaitre⁴⁰, E. Lemos Cid³⁹, O. Leroy⁶, T. Lesiak²⁷, B. Leverington¹²,
 P.-R. Li⁶³, T. Li³, Y. Li⁷, Z. Li⁶¹, T. Likhomanenko⁶⁸, R. Lindner⁴⁰, F. Lionetto⁴²,
 V. Lisovskyi⁷, X. Liu³, D. Loh⁵⁰, A. Loi¹⁶, I. Longstaff⁵³, J.H. Lopes², D. Lucchesi^{23,o},
 M. Lucio Martinez³⁹, H. Luo⁵², A. Lupato²³, E. Luppi^{17,g}, O. Lupton⁴⁰, A. Lusiani²⁴, X. Lyu⁶³,
 F. Machefert⁷, F. Maciuc³⁰, V. Macko⁴¹, P. Mackowiak¹⁰, S. Maddrell-Mander⁴⁸, O. Maev^{31,40},
 K. Maguire⁵⁶, D. Maisuzenko³¹, M.W. Majewski²⁸, S. Malde⁵⁷, A. Malinin⁶⁸, T. Maltsev^{36,w},
 G. Manca^{16,f}, G. Mancinelli⁶, P. Manning⁶¹, D. Marangotto^{22,q}, J. Maratas^{5,v}, J.F. Marchand⁴,
 U. Marconi¹⁵, C. Marin Benito³⁸, M. Marinangeli⁴¹, P. Marino⁴¹, J. Marks¹², G. Martellotti²⁶,
 M. Martin⁶, M. Martinelli⁴¹, D. Martinez Santos³⁹, F. Martinez Vidal⁷⁰, D. Martins Tostes²,
 L.M. Massacrier⁷, A. Massafferri¹, R. Matev⁴⁰, A. Mathad⁵⁰, Z. Mathe⁴⁰, C. Matteuzzi²¹,
 A. Mauri⁴², E. Maurice^{7,b}, B. Maurin⁴¹, A. Mazurov⁴⁷, M. McCann^{55,40}, A. McNab⁵⁶,
 R. McNulty¹³, J.V. Mead⁵⁴, B. Meadows⁵⁹, C. Meaux⁶, F. Meier¹⁰, N. Meinert⁶⁷,
 D. Melnychuk²⁹, M. Merk⁴³, A. Merli^{22,40,q}, E. Michielin²³, D.A. Milanes⁶⁶, E. Millard⁵⁰,
 M.-N. Minard⁴, L. Minzoni¹⁷, D.S. Mitzel¹², A. Mogini⁸, J. Molina Rodriguez¹,
 T. Mombacher¹⁰, I.A. Monroy⁶⁶, S. Monteil⁵, M. Morandin²³, M.J. Morello^{24,t}, O. Morgunova⁶⁸,
 J. Moron²⁸, A.B. Morris⁵², R. Mountain⁶¹, F. Muheim⁵², M. Mulder⁴³, D. Müller⁵⁶, J. Müller¹⁰,
 K. Müller⁴², V. Müller¹⁰, P. Naik⁴⁸, T. Nakada⁴¹, R. Nandakumar⁵¹, A. Nandi⁵⁷, I. Nasteva²,
 M. Needham⁵², N. Neri^{22,40}, S. Neubert¹², N. Neufeld⁴⁰, M. Neuner¹², T.D. Nguyen⁴¹,
 C. Nguyen-Mau^{41,n}, S. Nieswand⁹, R. Niet¹⁰, N. Nikitin³³, T. Nikodem¹², A. Nogay⁶⁸,
 D.P. O'Hanlon⁵⁰, A. Oblakowska-Mucha²⁸, V. Obraztsov³⁷, S. Ogilvy¹⁹, R. Oldeman^{16,f},
 C.J.G. Onderwater⁷¹, A. Ossowska²⁷, J.M. Otalora Goicochea², P. Owen⁴², A. Oyanguren⁷⁰,
 P.R. Pais⁴¹, A. Palano^{14,d}, M. Palutan^{19,40}, A. Papanestis⁵¹, M. Pappagallo^{14,d},
 L.L. Pappalardo^{17,g}, W. Parker⁶⁰, C. Parkes⁵⁶, G. Passaleva¹⁸, A. Pastore^{14,d}, M. Patel⁵⁵,
 C. Patrignani^{15,e}, A. Pearce⁴⁰, A. Pellegrino⁴³, G. Penso²⁶, M. Pepe Altarelli⁴⁰, S. Perazzini⁴⁰,
 P. Perret⁵, L. Pescatore⁴¹, K. Petridis⁴⁸, A. Petrolini^{20,h}, A. Petrov⁶⁸, M. Petruzzo^{22,q},
 E. Picatoste Olloqui³⁸, B. Pietrzyk⁴, M. Pikies²⁷, D. Pinci²⁶, A. Pistone^{20,h}, A. Piucci¹²,
 V. Placinta³⁰, S. Playfer⁵², M. Plo Casasus³⁹, F. Polci⁸, M. Poli Lener¹⁹, A. Poluektov^{50,36},
 I. Polyakov⁶¹, E. Polycarpo², G.J. Pomery⁴⁸, S. Ponce⁴⁰, A. Popov³⁷, D. Popov^{11,40},
 S. Poslavskii³⁷, C. Potterat², E. Price⁴⁸, J. Prisciandaro³⁹, C. Prouve⁴⁸, V. Pugatch⁴⁶,
 A. Puig Navarro⁴², H. Pullen⁵⁷, G. Punzi^{24,p}, W. Qian⁵⁰, R. Quagliani^{7,48}, B. Quintana⁵,
 B. Rachwal²⁸, J.H. Rademacker⁴⁸, M. Rama²⁴, M. Ramos Pernas³⁹, M.S. Rangel², I. Raniuk^{45,†},
 F. Ratnikov³⁵, G. Raven⁴⁴, M. Ravonel Salzgeber⁴⁰, M. Reboud⁴, F. Redi⁵⁵, S. Reichert¹⁰,

A.C. dos Reis¹, C. Remon Alepuz⁷⁰, V. Renaudin⁷, S. Ricciardi⁵¹, S. Richards⁴⁸, M. Rihl⁴⁰,
 K. Rinnert⁵⁴, V. Rives Molina³⁸, P. Robbe⁷, A. Robert⁸, A.B. Rodrigues¹, E. Rodrigues⁵⁹,
 J.A. Rodriguez Lopez⁶⁶, P. Rodriguez Perez^{56,†}, A. Rogozhnikov³⁵, S. Roiser⁴⁰, A. Rollings⁵⁷,
 V. Romanovskiy³⁷, A. Romero Vidal³⁹, J.W. Ronayne¹³, M. Rotondo¹⁹, M.S. Rudolph⁶¹,
 T. Ruf⁴⁰, P. Ruiz Valls⁷⁰, J. Ruiz Vidal⁷⁰, J.J. Saborido Silva³⁹, E. Sadykhov³², N. Sagidova³¹,
 B. Saitta^{16,f}, V. Salustino Guimaraes¹, C. Sanchez Mayordomo⁷⁰, B. Sanmartin Sedes³⁹,
 R. Santacesaria²⁶, C. Santamarina Rios³⁹, M. Santimaria¹⁹, E. Santovetti^{25,j}, G. Sarpis⁵⁶,
 A. Sarti²⁶, C. Satriano^{26,s}, A. Satta²⁵, D.M. Saunders⁴⁸, D. Savrina^{32,33}, S. Schael⁹,
 M. Schellenberg¹⁰, M. Schiller⁵³, H. Schindler⁴⁰, M. Schlupp¹⁰, M. Schmelling¹¹, T. Schmelzer¹⁰,
 B. Schmidt⁴⁰, O. Schneider⁴¹, A. Schopper⁴⁰, H.F. Schreiner⁵⁹, K. Schubert¹⁰, M. Schubiger⁴¹,
 M.-H. Schune⁷, R. Schwemmer⁴⁰, B. Sciascia¹⁹, A. Sciubba^{26,k}, A. Semennikov³²,
 E.S. Sepulveda⁸, A. Sergi⁴⁷, N. Serra⁴², J. Serrano⁶, L. Sestini²³, P. Seyfert⁴⁰, M. Shapkin³⁷,
 I. Shapoval⁴⁵, Y. Shcheglov³¹, T. Shears⁵⁴, L. Shekhtman^{36,w}, V. Shevchenko⁶⁸, B.G. Siddi^{17,40},
 R. Silva Coutinho⁴², L. Silva de Oliveira², G. Simi^{23,o}, S. Simone^{14,d}, M. Sirendi⁴⁹,
 N. Skidmore⁴⁸, T. Skwarnicki⁶¹, E. Smith⁵⁵, I.T. Smith⁵², J. Smith⁴⁹, M. Smith⁵⁵,
 I. Soares Lavra¹, M.D. Sokoloff⁵⁹, F.J.P. Soler⁵³, B. Souza De Paula², B. Spaan¹⁰, P. Spradlin⁵³,
 S. Sridharan⁴⁰, F. Stagni⁴⁰, M. Stahl¹², S. Stahl⁴⁰, P. Steffko⁴¹, S. Stefkova⁵⁵, O. Steinkamp⁴²,
 S. Stemmler¹², O. Stenyakin³⁷, M. Stepanova³¹, H. Stevens¹⁰, S. Stone⁶¹, B. Storaci⁴²,
 S. Stracka^{24,p}, M.E. Stramaglia⁴¹, M. Straticiuc³⁰, U. Straumann⁴², J. Sun³, L. Sun⁶⁴,
 W. Sutcliffe⁵⁵, K. Swientek²⁸, V. Syropoulos⁴⁴, M. Szczekowski²⁹, T. Szumlak²⁸,
 M. Szymanski⁶³, S. T'Jampens⁴, A. Tayduganov⁶, T. Tekampe¹⁰, G. Tellarini^{17,g}, F. Teubert⁴⁰,
 E. Thomas⁴⁰, J. van Tilburg⁴³, M.J. Tilley⁵⁵, V. Tisserand⁴, M. Tobin⁴¹, S. Tolk⁴⁹,
 L. Tomassetti^{17,g}, D. Tonelli²⁴, F. Toriello⁶¹, R. Tourinho Jadallah Aoude¹, E. Tournefier⁴,
 M. Traill⁵³, M.T. Tran⁴¹, M. Tresch⁴², A. Trisovic⁴⁰, A. Tsaregorodtsev⁶, P. Tsopelas⁴³,
 A. Tully⁴⁹, N. Tuning^{43,40}, A. Ukleja²⁹, A. Usachov⁷, A. Ustyuzhanin³⁵, U. Uwer¹²,
 C. Vacca^{16,f}, A. Vagner⁶⁹, V. Vagnoni^{15,40}, A. Valassi⁴⁰, S. Valat⁴⁰, G. Valenti¹⁵,
 R. Vazquez Gomez¹⁹, P. Vazquez Regueiro³⁹, S. Vecchi¹⁷, M. van Veghel⁴³, J.J. Velthuis⁴⁸,
 M. Veltri^{18,r}, G. Veneziano⁵⁷, A. Venkateswaran⁶¹, T.A. Verlage⁹, M. Vernet⁵, M. Vesterinen⁵⁷,
 J.V. Viana Barbosa⁴⁰, B. Viaud⁷, D. Vieira⁶³, M. Vieites Diaz³⁹, H. Viemann⁶⁷,
 X. Vilasis-Cardona^{38,m}, M. Vitti⁴⁹, V. Volkov³³, A. Vollhardt⁴², B. Voneki⁴⁰, A. Vorobyev³¹,
 V. Vorobyev^{36,w}, C. Voß⁹, J.A. de Vries⁴³, C. Vázquez Sierra³⁹, R. Waldi⁶⁷, C. Wallace⁵⁰,
 R. Wallace¹³, J. Walsh²⁴, J. Wang⁶¹, D.R. Ward⁴⁹, H.M. Wark⁵⁴, N.K. Watson⁴⁷,
 D. Websdale⁵⁵, A. Weiden⁴², M. Whitehead⁴⁰, J. Wicht⁵⁰, G. Wilkinson^{57,40}, M. Wilkinson⁶¹,
 M. Williams⁵⁶, M.P. Williams⁴⁷, M. Williams⁵⁸, T. Williams⁴⁷, F.F. Wilson⁵¹, J. Wimberley⁶⁰,
 M. Winn⁷, J. Wishahi¹⁰, W. Wislicki²⁹, M. Witek²⁷, G. Wormser⁷, S.A. Wotton⁴⁹,
 K. Wraight⁵³, K. Wyllie⁴⁰, Y. Xie⁶⁵, Z. Xu⁴, Z. Yang³, Z. Yang⁶⁰, Y. Yao⁶¹, H. Yin⁶⁵, J. Yu⁶⁵,
 X. Yuan⁶¹, O. Yushchenko³⁷, K.A. Zarebski⁴⁷, M. Zavertyaev^{11,c}, L. Zhang³, Y. Zhang⁷,
 A. Zhelezov¹², Y. Zheng⁶³, X. Zhu³, V. Zhukov³³, J.B. Zonneveld⁵², S. Zucchelli¹⁵.

¹Centro Brasileiro de Pesquisas Físicas (CBPF), Rio de Janeiro, Brazil

²Universidade Federal do Rio de Janeiro (UFRJ), Rio de Janeiro, Brazil

³Center for High Energy Physics, Tsinghua University, Beijing, China

⁴LAPP, Université Savoie Mont-Blanc, CNRS/IN2P3, Annecy-Le-Vieux, France

⁵Clermont Université, Université Blaise Pascal, CNRS/IN2P3, LPC, Clermont-Ferrand, France

⁶Aix Marseille Univ, CNRS/IN2P3, CPPM, Marseille, France

⁷LAL, Université Paris-Sud, CNRS/IN2P3, Orsay, France

⁸LPNHE, Université Pierre et Marie Curie, Université Paris Diderot, CNRS/IN2P3, Paris, France

⁹I. Physikalisches Institut, RWTH Aachen University, Aachen, Germany

¹⁰Fakultät Physik, Technische Universität Dortmund, Dortmund, Germany

¹¹Max-Planck-Institut für Kernphysik (MPIK), Heidelberg, Germany

¹²Physikalisches Institut, Ruprecht-Karls-Universität Heidelberg, Heidelberg, Germany

¹³School of Physics, University College Dublin, Dublin, Ireland

- ¹⁴Sezione INFN di Bari, Bari, Italy
¹⁵Sezione INFN di Bologna, Bologna, Italy
¹⁶Sezione INFN di Cagliari, Cagliari, Italy
¹⁷Universita e INFN, Ferrara, Ferrara, Italy
¹⁸Sezione INFN di Firenze, Firenze, Italy
¹⁹Laboratori Nazionali dell'INFN di Frascati, Frascati, Italy
²⁰Sezione INFN di Genova, Genova, Italy
²¹Universita & INFN, Milano-Bicocca, Milano, Italy
²²Sezione di Milano, Milano, Italy
²³Sezione INFN di Padova, Padova, Italy
²⁴Sezione INFN di Pisa, Pisa, Italy
²⁵Sezione INFN di Roma Tor Vergata, Roma, Italy
²⁶Sezione INFN di Roma La Sapienza, Roma, Italy
²⁷Henryk Niewodniczanski Institute of Nuclear Physics Polish Academy of Sciences, Kraków, Poland
²⁸AGH - University of Science and Technology, Faculty of Physics and Applied Computer Science, Kraków, Poland
²⁹National Center for Nuclear Research (NCBJ), Warsaw, Poland
³⁰Horia Hulubei National Institute of Physics and Nuclear Engineering, Bucharest-Magurele, Romania
³¹Petersburg Nuclear Physics Institute (PNPI), Gatchina, Russia
³²Institute of Theoretical and Experimental Physics (ITEP), Moscow, Russia
³³Institute of Nuclear Physics, Moscow State University (SINP MSU), Moscow, Russia
³⁴Institute for Nuclear Research of the Russian Academy of Sciences (INR RAN), Moscow, Russia
³⁵Yandex School of Data Analysis, Moscow, Russia
³⁶Budker Institute of Nuclear Physics (SB RAS), Novosibirsk, Russia
³⁷Institute for High Energy Physics (IHEP), Protvino, Russia
³⁸ICCUB, Universitat de Barcelona, Barcelona, Spain
³⁹Universidad de Santiago de Compostela, Santiago de Compostela, Spain
⁴⁰European Organization for Nuclear Research (CERN), Geneva, Switzerland
⁴¹Institute of Physics, Ecole Polytechnique Fédérale de Lausanne (EPFL), Lausanne, Switzerland
⁴²Physik-Institut, Universität Zürich, Zürich, Switzerland
⁴³Nikhef National Institute for Subatomic Physics, Amsterdam, The Netherlands
⁴⁴Nikhef National Institute for Subatomic Physics and VU University Amsterdam, Amsterdam, The Netherlands
⁴⁵NSC Kharkiv Institute of Physics and Technology (NSC KIPT), Kharkiv, Ukraine
⁴⁶Institute for Nuclear Research of the National Academy of Sciences (KINR), Kyiv, Ukraine
⁴⁷University of Birmingham, Birmingham, United Kingdom
⁴⁸H.H. Wills Physics Laboratory, University of Bristol, Bristol, United Kingdom
⁴⁹Cavendish Laboratory, University of Cambridge, Cambridge, United Kingdom
⁵⁰Department of Physics, University of Warwick, Coventry, United Kingdom
⁵¹STFC Rutherford Appleton Laboratory, Didcot, United Kingdom
⁵²School of Physics and Astronomy, University of Edinburgh, Edinburgh, United Kingdom
⁵³School of Physics and Astronomy, University of Glasgow, Glasgow, United Kingdom
⁵⁴Oliver Lodge Laboratory, University of Liverpool, Liverpool, United Kingdom
⁵⁵Imperial College London, London, United Kingdom
⁵⁶School of Physics and Astronomy, University of Manchester, Manchester, United Kingdom
⁵⁷Department of Physics, University of Oxford, Oxford, United Kingdom
⁵⁸Massachusetts Institute of Technology, Cambridge, MA, United States
⁵⁹University of Cincinnati, Cincinnati, OH, United States
⁶⁰University of Maryland, College Park, MD, United States
⁶¹Syracuse University, Syracuse, NY, United States
⁶²Pontifícia Universidade Católica do Rio de Janeiro (PUC-Rio), Rio de Janeiro, Brazil, associated to ²
⁶³University of Chinese Academy of Sciences, Beijing, China, associated to ³
⁶⁴School of Physics and Technology, Wuhan University, Wuhan, China, associated to ³
⁶⁵Institute of Particle Physics, Central China Normal University, Wuhan, Hubei, China, associated to ³
⁶⁶Departamento de Fisica , Universidad Nacional de Colombia, Bogota, Colombia, associated to ⁸
⁶⁷Institut für Physik, Universität Rostock, Rostock, Germany, associated to ¹²

⁶⁸*National Research Centre Kurchatov Institute, Moscow, Russia, associated to* ³²

⁶⁹*National Research Tomsk Polytechnic University, Tomsk, Russia, associated to* ³²

⁷⁰*Instituto de Fisica Corpuscular, Centro Mixto Universidad de Valencia - CSIC, Valencia, Spain, associated to* ³⁸

⁷¹*Van Swinderen Institute, University of Groningen, Groningen, The Netherlands, associated to* ⁴³

^a*Universidade Federal do Triângulo Mineiro (UFTM), Uberaba-MG, Brazil*

^b*Laboratoire Leprince-Ringuet, Palaiseau, France*

^c*P.N. Lebedev Physical Institute, Russian Academy of Science (LPI RAS), Moscow, Russia*

^d*Università di Bari, Bari, Italy*

^e*Università di Bologna, Bologna, Italy*

^f*Università di Cagliari, Cagliari, Italy*

^g*Università di Ferrara, Ferrara, Italy*

^h*Università di Genova, Genova, Italy*

ⁱ*Università di Milano Bicocca, Milano, Italy*

^j*Università di Roma Tor Vergata, Roma, Italy*

^k*Università di Roma La Sapienza, Roma, Italy*

^l*AGH - University of Science and Technology, Faculty of Computer Science, Electronics and Telecommunications, Kraków, Poland*

^m*LIFAELS, La Salle, Universitat Ramon Llull, Barcelona, Spain*

ⁿ*Hanoi University of Science, Hanoi, Viet Nam*

^o*Università di Padova, Padova, Italy*

^p*Università di Pisa, Pisa, Italy*

^q*Università degli Studi di Milano, Milano, Italy*

^r*Università di Urbino, Urbino, Italy*

^s*Università della Basilicata, Potenza, Italy*

^t*Scuola Normale Superiore, Pisa, Italy*

^u*Università di Modena e Reggio Emilia, Modena, Italy*

^v*Iligan Institute of Technology (IIT), Iligan, Philippines*

^w*Novosibirsk State University, Novosibirsk, Russia*

[†]*Deceased*